

LASER MICROABLATIVE TUNNEL FORMATION TO INITIATE ALVEOLAR BONE REGENERATION. PILOT *EX VIVO* STUDY

UDC 616.716.86.001.6–089:57

Received 07.11.2013



M.M. Karabut, Junior Researcher, Biotussie Optical Structure Research Laboratory, Scientific Research Institute of Biomedical Technologies¹; Postgraduate²;

A.V. Belikov, D.Phys.-Math.Sc., Professor, the Department of Laser Technology and Biomedical Optics³;

A.V. Skripnik, PhD, Associate Professor, the Department of Laser Technology and Biomedical Optics³;

T.V. Strunina, Researcher, the Department of Laser Technology and Biomedical Optics³;

S.S. Kuznetsov, D.Med.Sc., Professor, the Department of Pathological Anatomy¹;

E.B. Kiseleva, Junior Researcher, Biotussie Optical Structure Research Laboratory, Scientific Research Institute of Biomedical Technologies¹;

E.V. Gubarkova, Junior Researcher, Biotussie Optical Structure Research Laboratory, Scientific Research Institute of Biomedical Technologies¹; Postgraduate²;

I.V. Senina-Volzhskaya, PhD, Associate Professor, the Department of Dentistry, the Faculty of Doctors' Advanced Training¹;

F.I. Feldchtein, PhD, Consultant⁴;

G.B. Altshuler, D.Phys.-Math.Sc., Scientific Consultant⁴;

N.D. Gladkova, D.Med.Sc., Professor, Deputy Director for Science, Scientific Research Institute of Biomedical Technologies, Head of Biotussie Optical Structure Research Laboratory, Scientific Research Institute of Biomedical Technologies¹

¹Nizhny Novgorod State Medical Academy, Minin and Pozharsky Square, 10/1, Nizhny Novgorod, Russian Federation, 603000;

²Nizhny Novgorod State University named after N.I. Lobachevsky — National Research University, Gagarin Avenue, 23, Nizhny Novgorod, Russian Federation, 603950;

³St. Petersburg National Research University of Information Technologies, Mechanics and Optics, Kronverkskiy pr., 49, Saint Petersburg, Russian Federation, 197101;

⁴Dental Photonics, Inc., 1600 Boston-Providence Highway, Walpole 02081, USA

In recent years there has been demonstrated the ability of Erbium (Er) laser to cause effective ablation of bone tissue with minimum collateral damage. Non-surgical treatment of periodontitis using Er laser improves probing depth and clinical attachment level. However, periodontal anti-inflammatory therapy should not be limited to these parameters, but also should initiate tissue regeneration including bone tissue damaged by the disease.

The aim of the investigation was to evaluate feasibility and characterize the process of laser microablative tunnel formation in gingiva and alveolar bone using a pulse-periodic, single mode Er laser, and determine laser parameters providing appropriate size of the tunnel and coagulation zone needed to initiate healing and regeneration of the alveolar bone.

Materials and Methods. *Ex vivo* pig jaw was used as a model for the study. To create a through-gingiva microperforation of the alveolar bone, we used a laboratory prototype of Er laser and delivery system Alta PE-AT (Dental Photonics, Inc.).

Results. We performed a microperforation of a 1 mm thick gingiva and created a microcrater (tunnel) in the underlying bone using a single pulse with energy 5, 10 and 30 mJ. The laser tunnel characteristics in the gingiva, bone and dentine were characterized as a function of laser irradiation parameters. Optical microscopy and histology examination did not reveal carbonization or significant collateral damage of the bone tissue.

Conclusion. Using a laboratory prototype of Alta PE-AT Er laser we demonstrated feasibility of through gingiva laser microperforation of alveolar bone that can serve as the first step towards further study of healing and initiation of the alveolar bone regeneration.

Key words: microablative tunnel; alveolar bone regeneration; periodontitis; laser treatment; microperforation; Er laser.

For contacts: Gladkova Nataliya Dorofeevna, phone: +7951-910-66-57; e-mail: natalia.gladkova@gmail.com

The use of lasers as an alternative or adjunctive tool in periodontal therapy has gained enormous popularity in dental practice [1, 2]. Such laser advantages as hemostatic and bactericidal effects provide the improvement of treatment results [3, 4]. The following laser parameters are of great importance: wavelength, pulse energy and repetition rate, power, exposure time, as well as laser beam parameters, since they determine light absorption and light-tissue interactions [5]. The most attractive for periodontics is Erbium (Er) laser based on various crystals with wavelength of 3 μm (e.g., Er:YAG, Er:YSSG, Er:YLF, Er:YAP) [6] due to high absorption in hard and soft tissues and minimal thermal side effects [7]. A number of studies have demonstrated Er laser capability to remove effectively calcified debris and lipopolysaccharides on tooth root surface, as well as its antimicrobial effect [3, 8, 9]. Moreover, nonsurgical periodontal therapy using Er laser can result in significant clinical improvement as evidenced by decreased pocket depth and improved clinical attachment level [10, 11]. Er laser can also be used in combination with conventional surgical approaches [8, 12, 13]. Note that this laser type is the most appropriate for hard tissue treatment due to high absorption of its radiation by water and hydroxyapatites. In addition, the main bone components such as organic matrix and inorganic calcium salts also have very high absorption level for such radiation. Er laser capacity to cause effective hard tissue ablation with minimal collateral damage and, in particular, bone tissues with minimal collateral damage has been proven by a number of researchers [14, 15].

The primary purpose of periodontal therapy is to arrest an inflammatory process, which in its turn stops disease progression. However, to achieve the best effect periodontal therapy should also initiate regeneration of tissues damaged by the disease [16]. Thus, initiation of periodontal tissue regeneration is a critical goal of periodontal disease therapy.

In periodontal disease and gingivitis, both soft and hard tissues of oral cavity are known to be affected. Periodontitis manifests itself as progressive destruction of alveolar bone [17]. Conventional non-surgical treatment of destructive periodontal diseases aims mainly at inflammation elimination, but not the regeneration of bone or connective tissue damaged during the course of the disease [16]. In osseous tissue loss it is also useful to induce alveolar bone regeneration. Currently, the loss in osseous tissue is generally treated by transplantation [18] or guided tissue regeneration [19]. There are a number of techniques, which enable to induce bone regeneration. They include autogenic and heterogeneous bone grafts, the use of growth factors (mainly, bone morphogenetic proteins), polymer membranes using enamel matrix protein, as well as low intensity laser therapy application [20].

We have proposed to induce bone tissue regeneration using fractional laser microablation similar to the technique used for soft tissues — skin and mucosa. In previous works of our research team [21, 22] single laser microcoagulation fractional treatment was shown to induce oral mucosa regeneration that enables to consider the method as prospective treatment modality for gingival and periodontal diseases. As far as we know, no researches on bone tissue

regeneration induced by laser microdamages have ever been performed.

Alveolar bone is the most blood supplied bone tissue in human body; therefore, it can serve as the best object to demonstrate a new regeneration mechanism. Skin regeneration effect without scarring is observed in the formation of ablation columns, less than 0.3 mm in diameter, with coagulation zone width being less than 0.1 mm [23]. One might assume that in one tissue ablation, column parameters to initiate regeneration of tissue with normal morphology are in the same range. In addition, it is important that a column is to be formed through gingiva requiring no flap surgery. Thus, the essential pre-requisite for implementation of the suggested concept of alveolar bone regeneration is laser microablative column (a laser tunnel, laser crater) formed on gingival surface and penetrating through the bone to tooth root surface (cement).

The aim of the investigation was to assess the capabilities of laser microablative tunnel formation in gingival and alveolar bone using a pulse-periodic single mode Er laser, determine laser parameters providing the dimensions of a tunnel and its coagulation layer necessary to initiate alveolar bone healing and regeneration.

Materials and Methods. We used *ex vivo* pig jaw as an animal model. Mandibular tissues were exposed to laser irradiation during the first 12 h after animal butchering.

The research consisted of three independent stages. Stage I aimed at the study of topography and structure of alveolar part of pig mandible on buccal side including gingival margin, alveolar bone, periodontal ligament, cement and dentine to choose an optimal place for the laser treatment. Stage II aimed at matching an appropriate laser mode (optimal combination of energy and number of laser pulses) to create microablation column in pig jaw formed through mucosa and in the alveolar bone causing minimal damage of surrounding tissues. The purpose of stage III was to study the condition of alveolar bone and dental tissue after laser treatment supported by morphological studies. For each stage of the experiment we prepared new intact pig mandibular specimens including its molar part consisting of 7 posterior teeth (2 premolars and 5 molars) (Fig. 1, a).

At the stage I of the experiment we performed longitudinal cutting of jaw fragment at premolar level, which enabled to determine topography and structure of alveolar part of pig mandible including gingival margin, alveolar bone, periodontal ligament, cement and dentine (Fig. 1, b–d). The study enabled to state that microablative laser treatment is to be performed at least 4–5 mm away from gingival margin to reach bone tissue.

The characteristics of the first laboratory prototype of laser and delivery system Alta PE-AT (Dental Photonics, Inc., USA) used in the study are represented in a table.

External water spray irrigation in the course of laser treatment was not performed.

Laser irradiation of laser prototype Alta PE-AT was focused on the gingival surface at the level of 8 mm apically from gingival margin on buccal side (Fig. 2).

Stage II of the experiment. Laser pulse energy (E_p) and the number of laser pulses (N_p) irradiating the gingival

surface varied. Laser pulse energy was 5, 10 and 30 mJ. The number of laser pulses for each of energies was 5, 7, 10 and 50. We took photos of laser treated gingiva using optical microscope ($\times 4$ objective). After photographic recording gingiva was mechanically separated from the hard tissue and without formalin fixation was nitroblue tetrazolium chloride (NBTc) stained for morphological study, which assessed the size of microcolumns formed in gingiva and the degree of collateral damage (macroscopic

visual evaluation, without preparing histologic slides). Hard tissue (alveolar bone, periodontal ligament, cement and dentine) was mechanically grinded off till the middle of laser microcrater to study its dimensions.

A total of 48 microablative columns were examined during stage II of the experiment: there were formed 4 microablative columns for each combination of energy and number of laser pulses (12 combinations).

Stage III of the experiment: the research objects (See

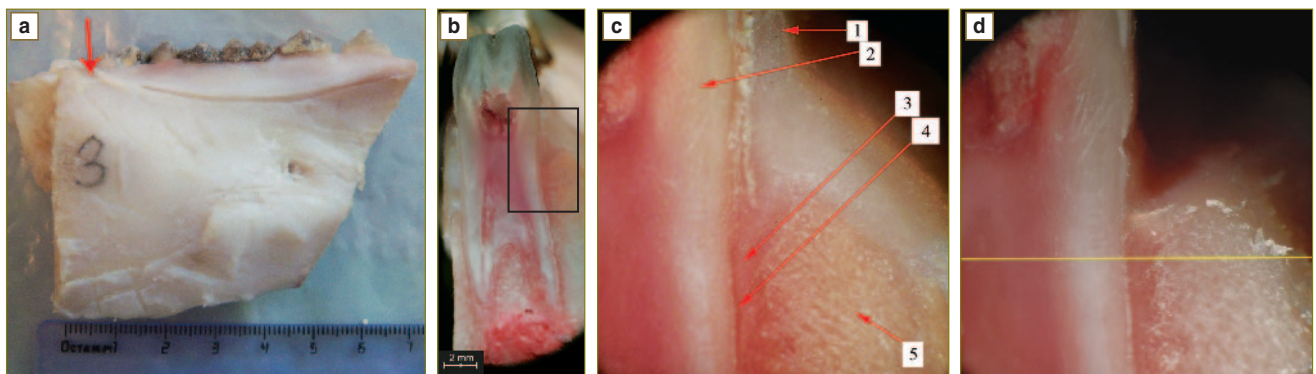


Fig. 1. Pig mandible fragment: *a* — an arrow indicates length cut level; *b* — length cut at premolar level (selected area is enlarged in Fig. *c* and *d*); *c* — the area including gingiva (1), dentine (2), periodontal ligament (3), cement (4) and alveolar bone (5); *d* — the same area after gingival removed. A yellow line — the level, at which further laser treatment was provided, and where histologic section shown in Fig. 8 was made

Principal technical characteristics of laboratory prototype of single mode (TEM₀₀) Erbium laser Alta PE-AT

Active medium type	Er:YAG
Laser wavelength, μm	2.94
Laser operation	Free-running pulse-periodic, single-mode(TEM ₀₀)
Pulse repetition rate, Hz	1
Pulse duration, μs :	
By the base	125 ($\pm 10\%$)
Half-width	105 ($\pm 10\%$)
Laser target exposure	Noncontact, through lens
Lens focal length, mm	~ 38
Laser beam size in lens focus, μm	~ 200
Irradiation energy at the site of treatment, mJ	Up to 30

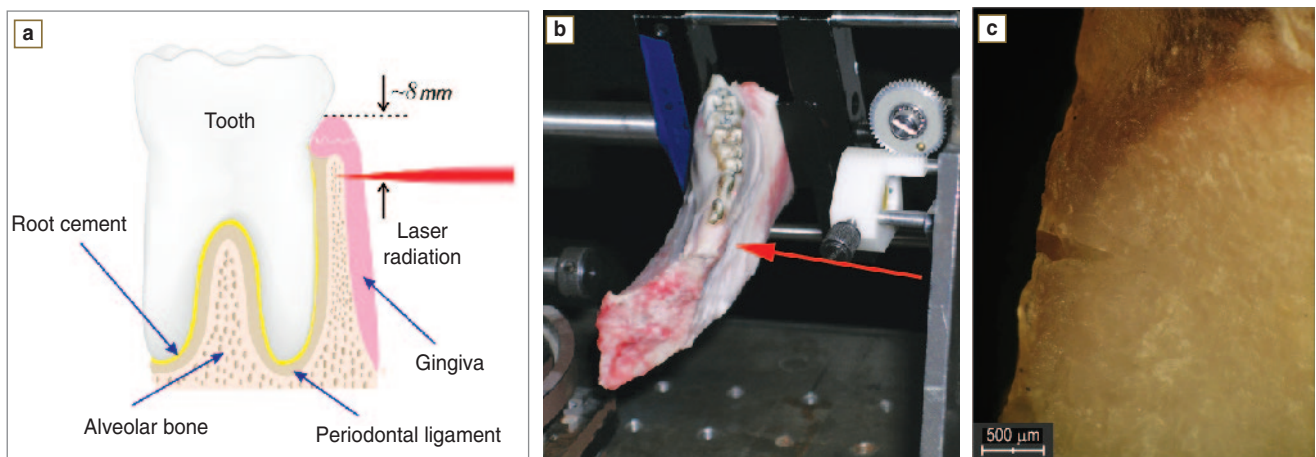


Fig. 2. Scheme (*a*), experiment photo (*b*) and photo of a specimen after laser treatment (*c*). An arrow indicates laser irradiation direction

Fig. 1, a) were exposed to laser irradiation according to the same schedule (See Fig. 2). Proper laser exposure was performed as one-place usage of series of 7 pulses with pulse energy of 5 mJ. Three columns under three teeth were formed. In addition, for convenience of further recognition, we made a laser marker with energy of 30 mJ and 7 pulses, which was located 4 mm coronally from the proper laser treatment (5 mJ). Therefore, the marker was separated from the gingival margin by a 4 mm-distance.

Histologic specimens were prepared in the following way: fragments, 1.5×1.5 cm in size, were sawed out of the whole jaw (including gingiva) up to 3 mm deep (to a tooth). A laser microcrater and a marker were located in the middle of the sawed fragment. The fragments were fixed in 10%-formaldehyde solution for 24 h, and in decalcifying fluid containing nitric acid for 6 days. After a series of flushes and fixation, the material was embedded in paraffin at 62°C for 48 h. The blocks were arranged in such a way that subsequently we could have histological cross sections of alveolar sockets including a tooth, which were along a laser column. Histologic bone specimens were hematoxylin-eosin stained with further observation under an optical microscope Leica DMLS (Germany) with magnification of 50, 100, 200, 400 and digital photography using the camera Nikon COOLPIX 5000 (Japan). It is significant that the principal task of a morphological stage of the experiment was the assessment of bone tissue alterations under laser irradiation. The preservation of mucosa on preparations was not critical.

Results. As mentioned above, *stage I of the experiment*

enabled to state accurately the topography of the mandible test area, which showed that laser microablative column should be formed at a distance of at least 4–5 mm from gingival margin to reach the alveolar bone.

At stage II of the experiment we determined laser action to result in through gingival tissue perforation and crater formation in bone tissue (Fig. 3 and 4). In a number of cases, we observed carbonization on soft tissue surface, characteristic of a large number of laser pulses ($N_p=50$), it was associated with tissue dehydration due to multiple exposure to laser irradiation (See Fig. 3). It is worth noting that there was no carbonization of gingival surface for all laser pulse energies used, if the number of pulses did not exceed 10 (Fig. 3).

A microablation column resulted from laser treatment consisted of a through-hole (microcolumn) in gingiva (Fig. 5) and microcrater in underlying bone tissue (Fig. 6) at a distance of 8 mm from gingival margin. In any combination of energy and number of laser pulses, gingival tissue (the thickness of gingival in treatment area was about 1 mm) was perforated through, i.e. even single mode laser irradiation with energy of 5 mJ and the number of pulses equal to 5 is able to perforate through soft gingival tissue 1 mm thick and reach bone tissue of pig jaw. Note that microcolumns in gum tissue extend in the part exposed to bone tissue, i.e. grow in diameter. This phenomena can be explained by additional ablation by laser beam or laser-induced acoustic energy reflected from gum-bone, and ablation action of the products of bone tissue laser damage on soft tissue. One should note extremely minor

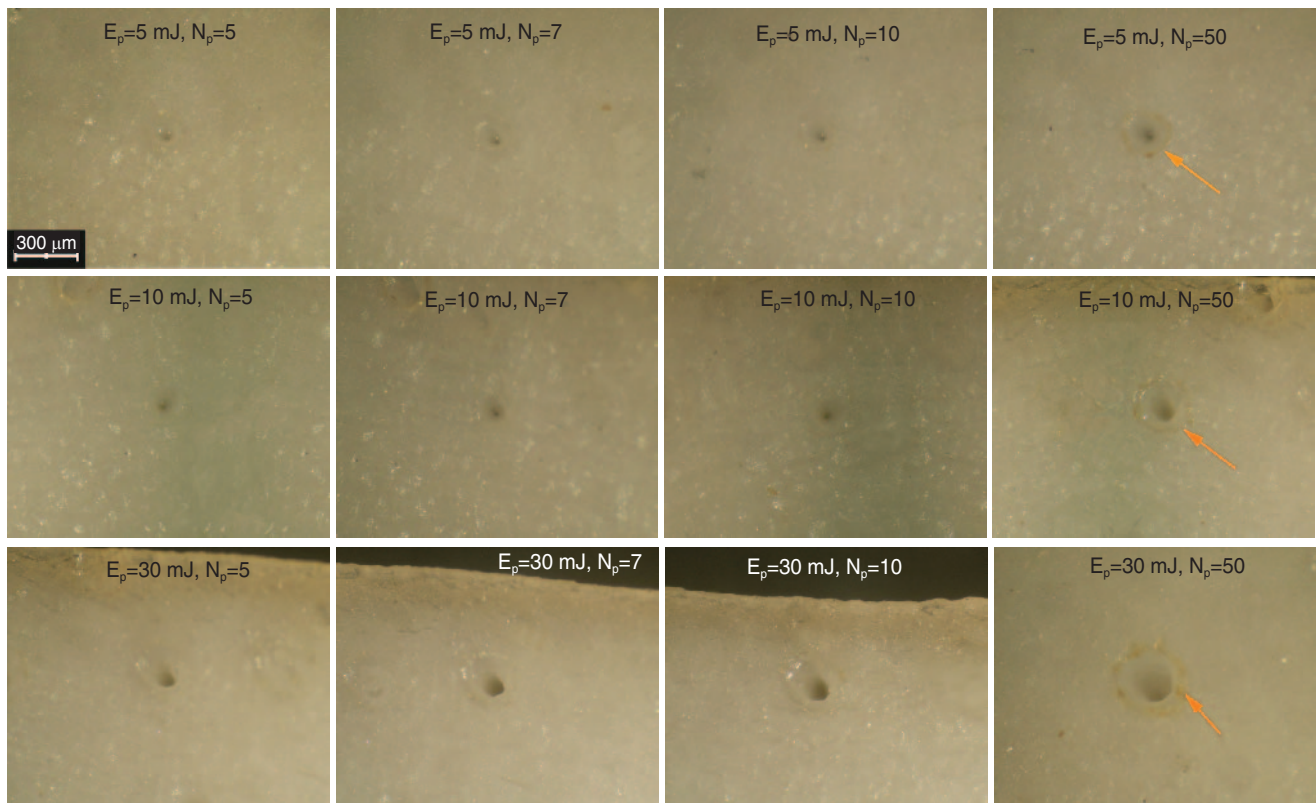


Fig. 3. Appearance of laser treatment areas on frontal surfaces of gingival tissue; ×4. The arrows indicate insignificant carbonization signs

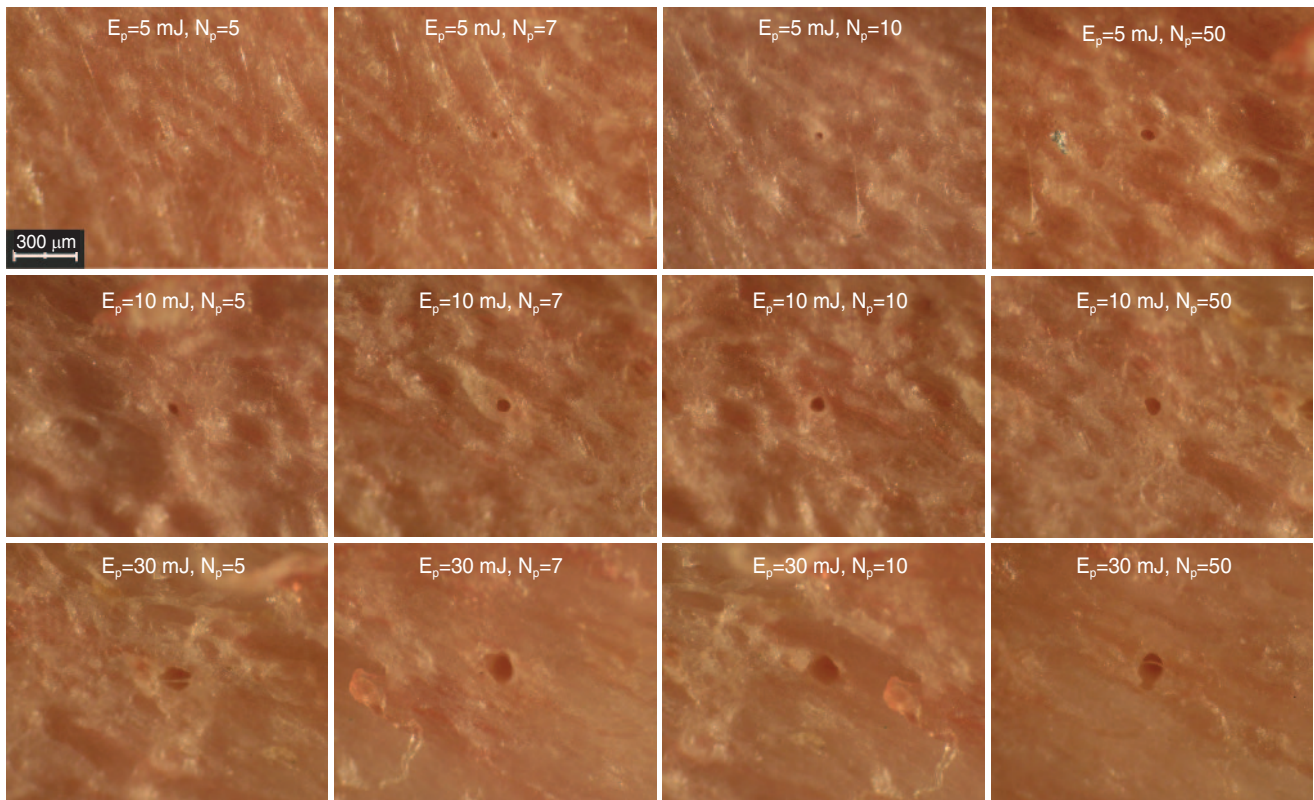


Fig. 4. Appearance of laser treatment areas on bone tissue surface located immediately below irradiated gingival tissue; $\times 4$

area of collateral damage of soft tissues surrounding a microcolumn, the damage being determined by NBTC stain loss, indicating tissue viability loss. The width of collateral damage determined macroscopically at magnification $\times 4$ depends on energy (E_p) and the number of laser pulses (N_p). If $E_p=5$ mJ and $N_p=5$, collateral damage width in the microcolumn wall is 10–20 μm , and if $E_p=30$ mJ and $N_p=50$, it reaches 40–50 μm .

Fig. 6 shows saw-cuts of alveolar bone after laser treatment in for different energy and number of pulses. Alveolar bone thickness at the place of laser crater formation is about 1 mm. Note that in some cases microcrater walls in alveolar bone had carbonization typical of a large number of laser pulses ($N_p=50$). As mentioned above, carbonization can be related to tissue dehydration under multiple laser irradiations. The problem is most likely to be resolved if gingival surface is externally sprayed by water during laser treatment. It is worth noting that there is no carbonization of gingival surface for all laser pulse energies used, if the number of pulses does not exceed $N_p=10$. It has been found that microcrater formation in alveolar bone needs $E_p=5$ mJ and $N_p=5-7$.

We measured the external diameter of a laser crater for various laser settings, when a crater is formed both in gingival and bone tissues. The diameters were found to increase with the growth of E_p and N_p . In experiment, the diameter of microcolumns in gingiva was within the range of 60–450 μm , and the diameter of microcraters in bone tissue — in the range 50–250 μm .

The assessment of the dependence of microcrater depth in pig jaw hard tissue on laser pulse energy E_p in different

N_p values showed crater depth to increase with the growth of E_p and N_p . In the experiment, microcrater depth in pig jaw hard tissue varied within the range of 200–1000 μm .

Thus, at stage II we determined the settings (energy and number of pulses) to form a microablation column in a pig jaw. We found that for soft tissue perforation and microcrater formation in alveolar bone it was sufficient to affect gingiva using energy of 5 mJ and the number of pulses equal to 5–7.

At stage III we used this particular minimum-energy laser setting, since it could provide through perforation of gingival tissue with the following destruction of the underlying bone.

Fig. 7 represents digital photos of laser jaw microperforation taken using the mode of 7 pulses and energy of 5 and 30 mJ. Microperforation diameter in alveolar bone exposed to 7 pulses with the energy of 5 mJ is comparable (and sometimes even lower) with the impression in the bone of periosteal processes after gingival removal (Fig. 7, a). It significantly complicates the identification of such a small-diameter microcolumn on histological section. For this reason, in the zone of morphological study at a distance of 4 mm from gingival margin there was a marker obtained with laser irradiation of 30 mJ and 7 pulses.

Morphological macroscopic study of experimental material showed the alteration of mucosa seen with the unaided eye in the form of small craters corresponding to laser markers. Microablative columns were not seen with the naked eye. Using $7\times$ magnifier, on mucosa there were seen round-shaped point defects, 150–200 μm in diameter. No alterations were revealed in the surrounding mucosa using low magnification. Incision of mucosa and

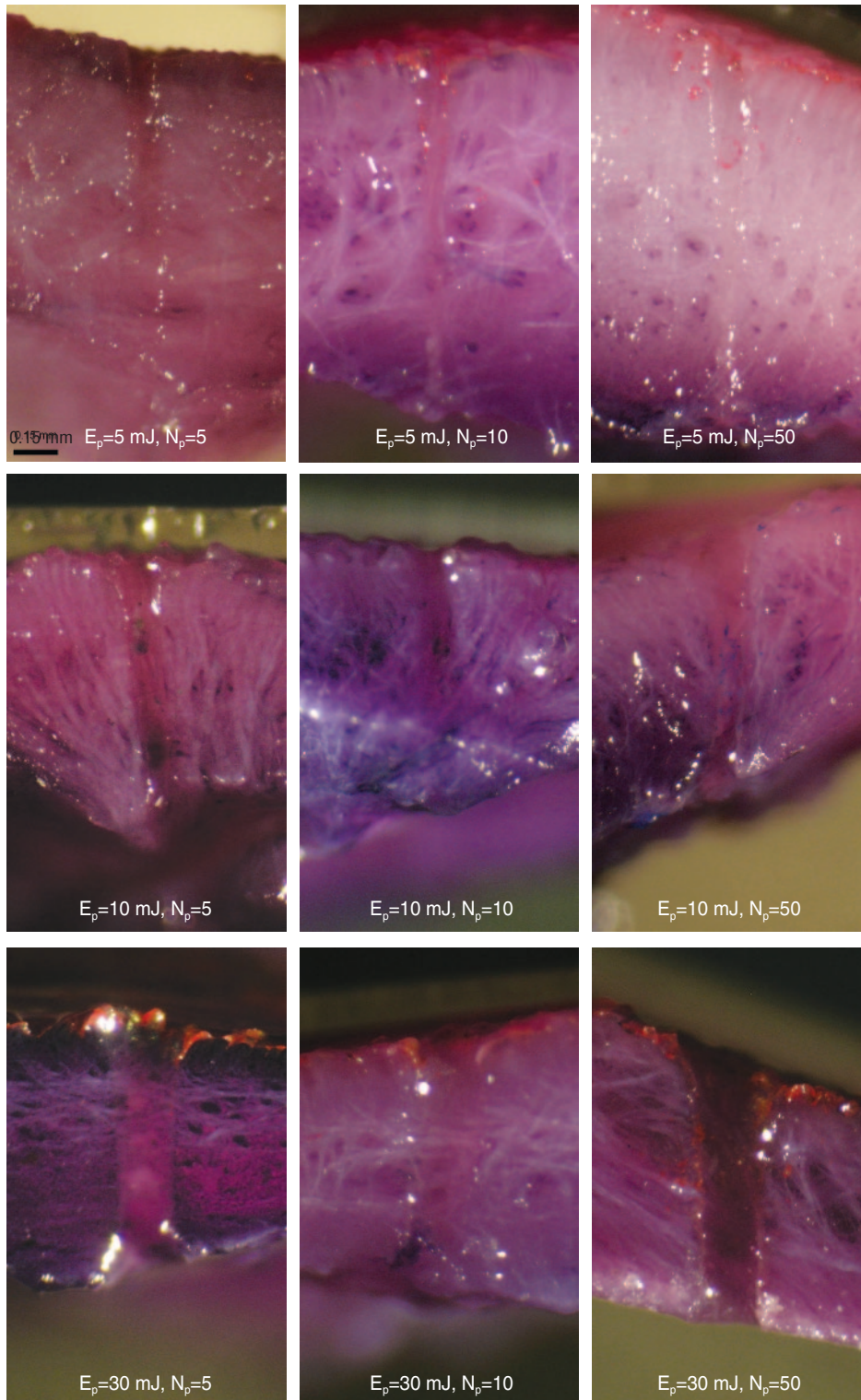


Fig. 5. Photos of vertical sections of microcolumns (nitroblue tetrazolium chloride staining, whole mount with longitudinal section) formed in pig jaw under exposure of Alta PE-AT. Bar size — 150 μ m, $\times 4$

underlying soft tissues (fibrous gingival tissue) showed no changes. After gingiva removal, on bone surface using 7-power magnifier we found only microcraters, 300–400 μ m in diameter, corresponding to laser markers. Surrounding bone tissue had no visible changes.

Bone tissue is known to consist of mineral and organic components including 30%, 60% and 10% of mass of organic, mineral and water components respectively. Mineral component provides strength and predominantly consists of calcium, phosphorus and microelements. Ostein

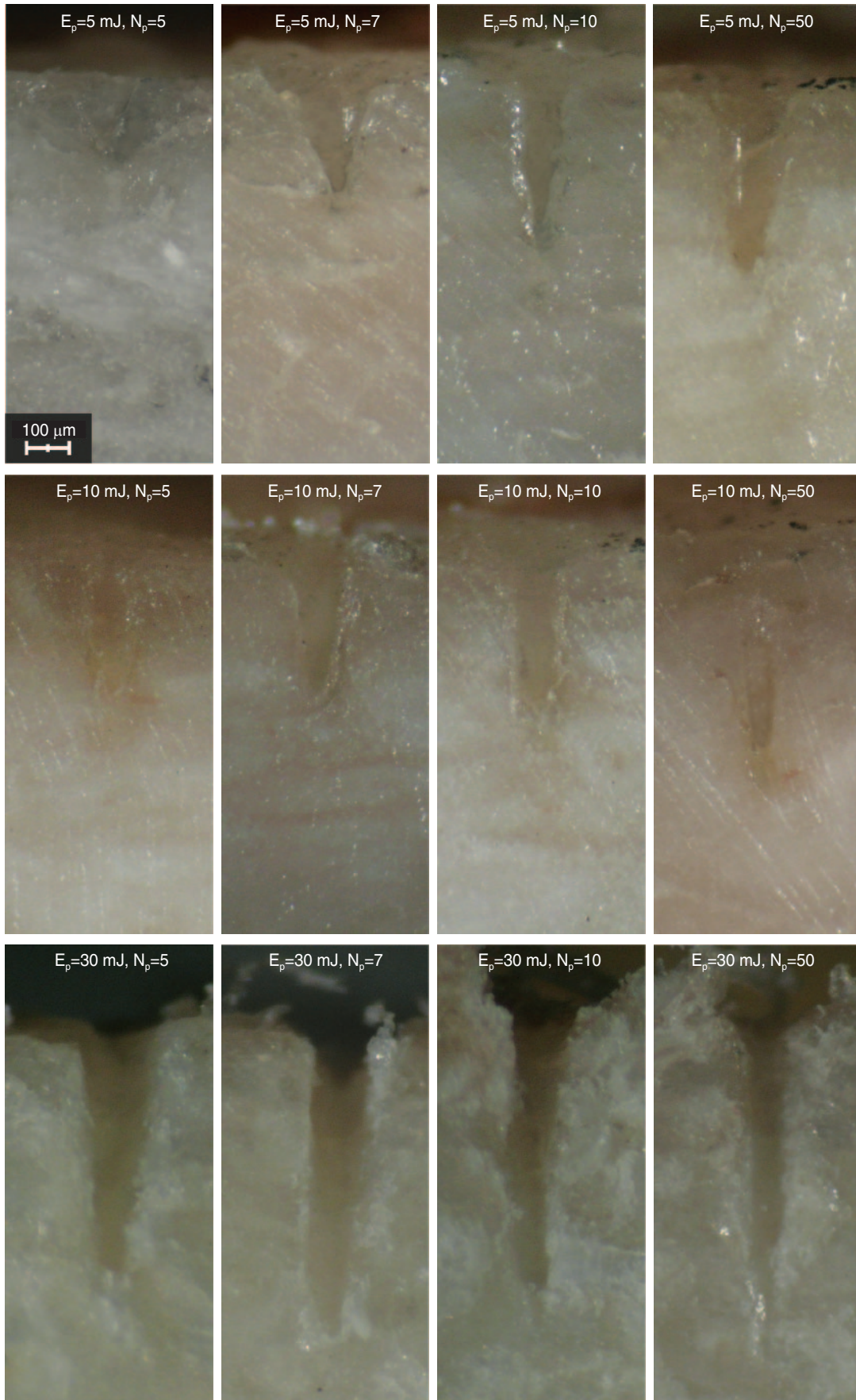


Fig. 6. Photos of vertical cuts of microcraters in alveolar bone at laser treatment site; $\times 4$

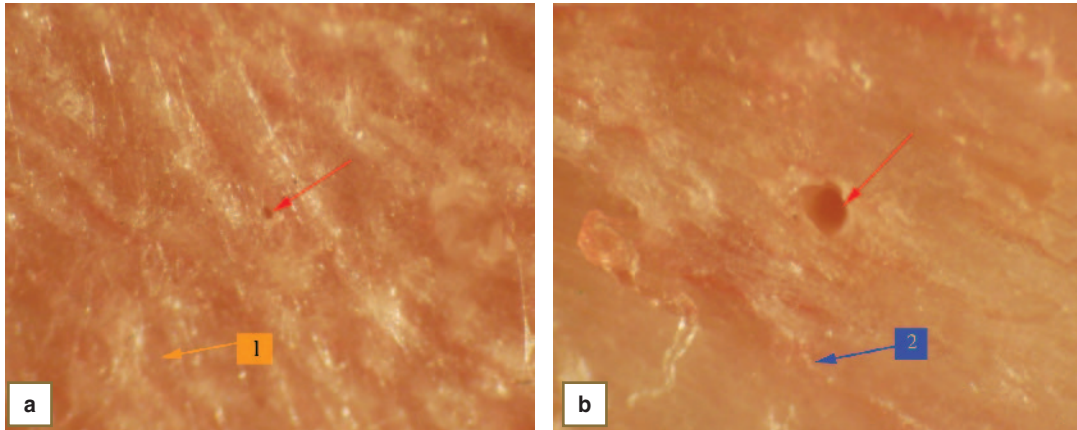


Fig. 7. Detailed view of bone tissue area with laser perforation using the mode of 7 pulses and energy of 5 mJ (a), and 7 pulses and energy of 30 mJ (b). Gingival tissue is removed from bone tissue surface. An arrow indicates microperforation area. 1 — surface irregularities, the points of periosteal processes penetration into bone; 2 — residual periosteal fibers

in the main organic component (type I collagen) making the bone more elastic. Bone is a complex of nanometer-sized carbonized apatite crystals in organic matrix of collagen fibers with highly hierarchical structure. Primary amino acid sequence in collagen molecule is identical in bones and other connective tissues; however, bone collagen has special profile of cross-links, which determine specific structure and physical properties of this protein in bone.

Cross section of intact pig mandibular tissue at a distance of 8 mm from gingival margin (Fig. 8) — just where laser microablative columns were formed — includes the following: anterior wall of tooth socket (periosteum, compact and trabecular bones), periodontal ligament, cement, dentine and tooth pulp. The Figure illustrates the thickness range of structures we revealed in 60 histological slides studied.

Tooth socket wall presents special type of bone tissue — alveolar bone characterized by thin periosteum consisting of two layers (outer fibrous and inner cambial layers), and a very thin compact lamina (Fig. 9, a). The basic part is spongy (trabecular or alveolar) layer. The thickness of intact tooth socket in our study varied greatly depending on the distance from gingival margin — from 1 to 3 mm. Spongy layer of alveolar bone includes trabecula and intertrabecular spaces. Osteoid forms the basis of bone trabecula. Osteoid is a bone substance consisting of collagen fibers and containing osteocytes. Histological staining makes osteoid show eosinophilic properties, though occasionally one can observe basophilic “stripes” with indistinct boundaries (“cement lines”) on low basophilic background of intercellular substance.

Trabecula of spongy substance are orderly arranged, along functional compression and expansion lines. Trabecula thickness varies largely — 100–250 μm. Intertrabecular spaces are filled by fibrous connective tissue closely adjacent to bone surface and separated from it by an osteoblast layer forming endost (See Fig. 9, a). Intertrabecular spaces vary in their size within great ranges (20–200 μm), and are characterized by disordered arrangement on histologic specimens. On the tooth side,

the bone is connected with a round periodontal ligament supporting a tooth due to connective tissue fiber bundles penetrating the bone (See Fig. 8).

Fig. 9, b demonstrates a laser column formed in the experiment using laser mode of 7 pulses with energy of



Fig. 8. Transverse section of an intact pig jaw at 8 mm-distance from gingival margin after mechanical removal of mucosa: 1 — periosteum, 0.11–0.22 mm; 2 — spongy bone, 1.22–3.50 mm; 3 — periodontal ligament, 0.42–0.69 mm (with papillae); 4 — cement, 0.30–0.34 mm; 5 — dentin, 1.0–1.2 mm; 6 — tooth, 1.0–1.5 mm. Frame size — 2.53×3.81 mm; staining — hematoxylin-eosin

30 mJ (laser marker). Laser treatment area on histologic specimen of alveolar bone looks like an elongated defect (a microcrater, tunnel, column), 430 μm in diameter and 2.1 mm deep. There are no structures inside a microcrater, except heavily deformed and deeply thinned discrete trabecula, which appear as compressed, "melting" structure. There were no cell elements (osteoblasts and osteoclasts) found. In collateral area, around a column there were observed no coagulation signs of osteoid collagen fibers, and no changes in osteocytes.

Discussion. Bone regeneration occurs due to cell proliferation in periosteal cambial layer, pluripotent poorly

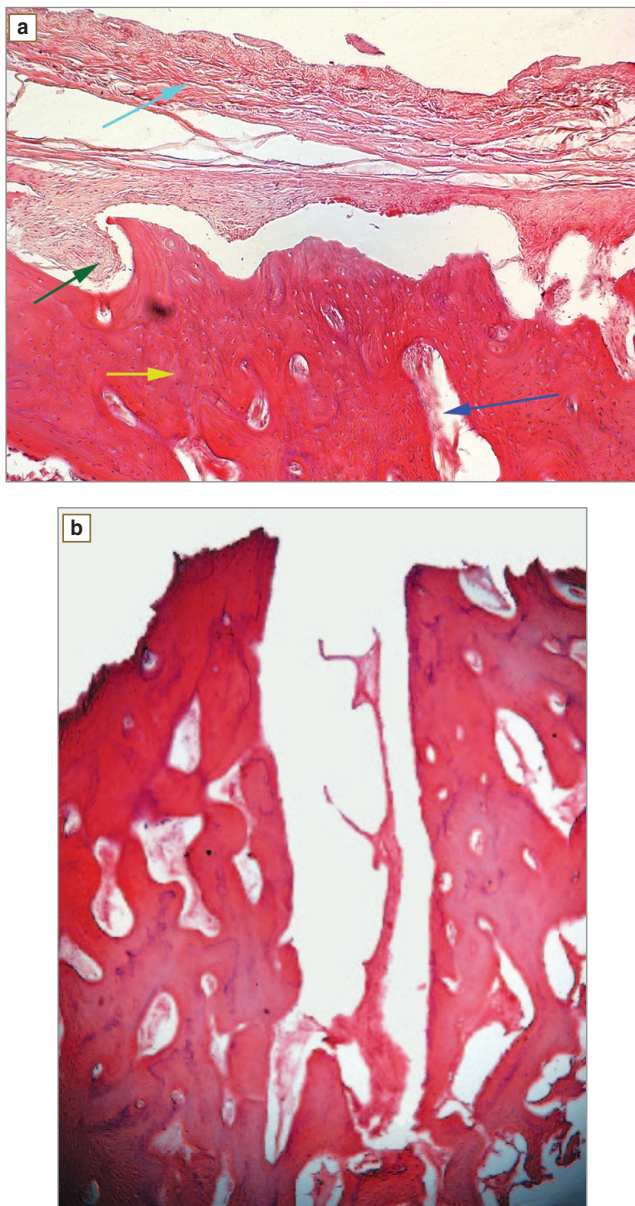


Fig. 9. Pig mandible spongy bone periosteum (a light blue arrow) and impressions of its processes on the bone (a dark green arrow); trabecula (a yellow arrow) and intertrabecular spaces (a blue arrow) (a), the size of frame — 650×490 μm ; a laser microablation column in a pig mandibular alveolar bone formed under the exposure of laser treatment of 7 pulses and energy of 30 mJ (b), the size of frame — 1960×2600 μm

differentiated cells of marrow stroma, endosteum, as well as due to mesenchymal cells of adventitia of ingrowing blood vessels. Four main stages can be distinguished in reparative regeneration process [24]:

- 1) proliferation and differentiation of cellular components;
- 2) creation and differentiation of bone structures;
- 3) creation of angiogenic bone structure;
- 4) reorganization of the primary regeneration and bone restitution.

The reparative regeneration is well studied. It takes 3–4 weeks in average and normally is described with weekly assessment of the histology data [25]. In 1 week after the damage, the defect is partially filled with blood components (mostly granulocytes and erythrocytes), fragments of loose connective tissue, where small islands of a new bone can be found. In 2 weeks the defect is already completely closed by a young bone tissue with a large number of full-filled blood on the periphery. In 3 weeks the defect is completely replaced by a newly created bone tissue. In 4 weeks the healing site can be only found by the traces of the osteolytic. By this time the bone structure is completely formed.

Several research groups have studied bone healing and regeneration after laser cutting. Regardless of laser type, bone healing after osteotomy, osteoplasty or bone implantation is known to be a complex process including local and systemic response, as well as the contribution of different cell types, enzymes, growth factors, cytokines and other signal proteins. Two studies [26, 27] compared the healing of tibia defects formed by rotation bur, CO₂- (780 and 1032 J/cm²) and Nd:YAG-lasers (714 and 1000 J/cm²) after osteotomy in rats. During the whole follow-up period (from 0 to 63 days after treatment), regardless of energy density and air/water flow used for surface cooling during the treatment, bone healing was greatly delayed. Severe collateral damage was the main factor, which affected the healing of laser-induced bone cut. Delayed healing was found to have a residual carbonized layer on the treated surface, some inert bone fragments encapsulated by fibrous connective tissue, necrotic bone parts and fragments surrounded by multinucleated giant cells [8, 9]. To form the holes, 0.4 mm in diameter, in maxilla and mandible of rabbits, other researchers in their study [28] used Er,Cr:YSGG-laser with energy density of 80 J/cm². Complete wound repair was observed on day 56 after treatment.

The sequence of events at an early healing stage consisting in inflammation and revascularization is of prime importance. Inflammatory stage is characterized by neutrophil migration with the following migration of macrophages to the defect. Macrophages play a key role in the initiation of tissue repair producing growth factors, which initiate angiogenesis, proliferation of fibroblasts, and maturation [14].

This study [14] included the comparative analysis of healing process of calvarial bone defects in rats after the treatment by Er:YAG-laser, CO₂-laser and after mechanical treatment. The defect area created by Er:YAG-laser was found to have more marked inflammatory cellular infiltration, fibroblast proliferation, and revascularization compared

to the tissues treated by a mechanical bur and CO₂-laser. 10 min after the treatment by Er:YAG-laser there was found an active migration of granulocytes and erythrocytes, forming aggregates of different density. The day after the treatment the red blood cell count decreased and number polymorphonuclear leukocytes and macrophages increased, especially close to the bone surface. By the third day, the number of neutrophils and fibroblasts increased. Moreover, there was phagocytosis and angiogenesis. Macrophages were seen in the maturing blood clot, especially close to bone surface. On day 7 histologic analysis revealed granulation tissue with fibroblasts and osteoblasts prevailing in the defect treated by Er:YAG-laser. Mineralization spots were found near the laser defect and even in the center of the defect in some specimens. There were observed collagen fibrils surrounding osteoblasts. 14-day follow up analysis showed much higher new bone tissue formation after Er:YAG-laser treatment compared to the treatment by mechanical bur and CO₂-laser treatment. There were observed osteoblast groups covering osteoid, and new bone tissue, as well as osteocytes built in the new bone. Thus, early bone healing after Er:YAG-laser treatment occurs more faster than after mechanical treatment by bur and CO₂-laser. It can be related to the fact that Er:YAG-laser treatment leads to minimal mechanical damage (compared to bur) and thermal injury (compared to CO₂-laser) of crater surface resulting in the formation of appropriate surface for cell attachment, therefore such laser treatment can be more effective in relation to the healing of bone tissue wounds [14].

Bone damage repair is known to depend mainly on the presence of osteoblast precursors in surrounding bone tissue, and the capability of these cells to penetrate into damage area and differentiate in osteoblasts. Other authors [28] demonstrated a positive effect of laser irradiation with 780 nm wavelength on initiation of femur defect regeneration in rats. A considerable amount of newly formed bone tissue within 15 days indicate biostimulation effect of laser therapy at early stages of regenerative process, which is characterized by a great number of cells, mainly osteoblasts and undifferentiated cells. The authors suspect an apparent biostimulating effect of laser irradiation, when these particular cells are treated [28].

The mechanisms initiating bone repair using laser irradiation are not yet completely understood, and they present complex processes including vascularization increase, collagen production, proliferation and differentiation of osteogenic cells, as well as DNA and RNA synthesis growth, i.e. impact on cell growth and protein synthesis, mitochondrial respiration and ATP synthesis [28]. Further studies have presented a new approach to the problem of initiating bone tissue regeneration by creating a pattern of laser microtunnels, less than 0.3–0.4 mm in diameter, surrounded by intact tissue. The healing process of such microdamage should occur rather quickly and result in healthy bone tissue formation. Thus, the described fractional laser treatment of alveolar bone damaged by periodontitis is expected to result in normal bone tissue regeneration.

Conclusion. The presented procedure of laser

microablation tunnel formation using a laboratory prototype of a single mode TEM₀₀ Erbium laser Alta PE-AT is the first step towards further study of the potential of alveolar bone healing and regeneration initiation. The applied technology of through gingiva microperforation of pig mandibular alveolar bone using a pulse-periodic single mode Er laser operating at 2.94 μm wavelength has shown the feasibility of such procedure. A perforation through the thickness of gingiva of about 1 mm and creation of a microcrater (tunnel) in the underlying alveolar tissue is possible with pulse energies of 5, 10 and 30 mJ. Macro- and microscopic study did not reveal any evident signs of the bone tissue carbonization.

The experiment has shown that for soft tissue perforation and microcrater formation in alveolar bone it was sufficient to perforate gingiva using energy of 5 mJ and 5–7 pulses. We have demonstrated the formation of microcraters 50–250 μm in diameter and up to 1 mm deep.

Laser damage area created at a distance of 4 mm from gingival margin with of 30 mJ and 7 pulses on histologic specimens of alveolar bone looks like microcrater with size 400 μm in diameter and 2.1 mm depth. Coagulation area of collateral damage in bone tissue does not exceed 10 μm.

Study Funding. The work was supported by Skolkovo Foundation grant No.MF-13-21 dated February, 6, 2013 “Development and commercialization of a modular laser system for periodontal treatment”.

Conflict of Interests. The authors have no conflict of interests to disclose.

Acknowledgments. The authors would like to express their sincere thanks to Natalia Yurievna Ignatyeva, D.Chem.Sc., and Professor Emil Naumovich Sobol for their contribution and fruitful discussion of the experimental results.

References

1. Ishikawa I., Sculean A. Laser dentistry in periodontics. In: Gutknecht N., editor. 1st International workshop of evidence based dentistry on lasers in dentistry. *Quintessence Publishing* 2007; 115–129.
2. Kreisler M., Al Haj H., d'Hoedt B. Clinical efficacy of semiconductor laser application as an adjunct to conventional scaling and root planing. *Lasers Surg Med* 2005 Dec; 37(5): 350–355.
3. Coleton S. Lasers in surgical periodontics and oral medicine. *Dent Clin North Am* 2004 Oct; 48(4): 937–962, vii.
4. Schwarz F., Aoki A., Becker J., Sculean A. Laser application in non-surgical periodontal therapy: a systematic review. *J Clin Periodontol* 2008 Sep; 35(8 Suppl): 29–44.
5. Manni J.G. *Dental applications of advanced lasers (DAAL)*. JGM Associates, Inc.; 2007.
6. Belikov A.V., Erofeev A.V., Shumilin V.V., Tkachuk A.M. Comparative study of the 3μm laser action on different hard tooth tissue samples using free running pulsed Er-doped YAG, YSGG, YAP and YLF lasers. *Dental Applications of Lasers* 1993; SPIE 2080: 60–77.
7. Aoki A., Mizutani K., Takasaki A.A., Sasaki K.M., Nagai S., Schwarz F., et al. Current status of clinical laser applications in periodontal therapy. *Gen Dent* 2008 Nov–Dec; 56(7): 674–687; quiz 688–689, 767.
8. Cobb C.M., Low S.B., Coluzzi D.J. Lasers and the treatment of chronic periodontitis. *Dent Clin North Am* 2010 Jan; 54(1): 35–53.
9. Cobb C.M. Lasers in periodontics: a review of the literature. *J Periodontol* 2006 Apr; 77(4): 545–564.

10. Sculean A., Chiantella G.C., Arweiler N.B., Becker J., Schwarz F., Stavropoulos A. Five-year clinical and histologic results following treatment of human intrabony defects with an enamel matrix derivative combined with a natural bone mineral. *Int J Periodontics Restorative Dent* 2008 Apr; 28(2): 153–61.
11. Gaspirc B., Skaleric U. Clinical evaluation of periodontal surgical treatment with an Er:YAG laser: 5-year results. *Journal of Periodontology* 2007 Oct; 78(10): 1864–1871.
12. Crespi R., Cappare P., Toscanelli I., Gherlone E., Romanos G.E. Effects of Er:YAG laser compared to ultrasonic scaler in periodontal treatment: a 2-year follow-up split-mouth clinical study. *J Periodontol* 2007 Jul; 78(7): 1195–1200.
13. Yoshino T., Aoki A., Oda S., Takasaki A.A., Mizutani K., Sasaki K.M., et al. Long-term histologic analysis of bone tissue alteration and healing following Er:YAG laser irradiation compared to electrosurgery. *Journal of Periodontology* 2009; 80(1): 82.
14. Pourzarandian A., Watanabe H., Aoki A., Ichinose S., Sasaki K.M., Nitta H., et al. Histological and TEM examination of early stages of bone healing after Er:YAG laser irradiation. *Photomed Laser Surg* 2004 Aug; 22(4): 342–350.
15. Hibst R. Lasers for caries removal and cavity preparation: State of the art and future directions. *J Oral Laser Appl* 2002; 2: 203–211.
16. Needleman I.G., Worthington H.V., Giedrys-Leeper E., Tucker R.J. Guided tissue regeneration for periodontal infra-bony defects. *Cochrane Database Syst Rev* 2006(2): CD001724.
17. Lukinykh L., Zhulev E., Chuprunova I. *Bolezni parodontia. Klinika, diagnostika, lechenie i profilaktika* [Periodontal diseases. Clinical picture, diagnosis, treatment and prevention]. Nizhny Novgorod: Izdatel'stvo Nizhegorodskoy gosudarstvennoy meditsinskoy akademii 2005; 322 p.
18. Verdugo F., D'addona A. Long-term stable periodontal regeneration by means of autologous bone grafting in patients with severe periodontitis. *Int J Periodontics Restorative Dent* 2012 Apr; 32(2): 157–164.
19. Needleman I., Tucker R., Giedrys-Leeper E., Worthington H. A systematic review of guided tissue regeneration for periodontal infrabony defects. *J Periodontol Res* 2002 Oct; 37(5): 380–388.
20. Pinheiro A.L., Martinez Gerbi M.E., de Assis Limeira F. Jr., Carneiro Ponzi E.A., Marques A.M., Carvalho C.M., et al. Bone repair following bone grafting hydroxyapatite guided bone regeneration and infra-red laser photobiomodulation: a histological study in a rodent model. *Lasers Med Sci* 2009 Mar; 24(2): 234–240.
21. Gladkova N.D., Karabut M.M., Kiseleva E.B., Fomina Y.V., Muraev A.A., Balalaeva I.V., Feldstein F.I. Prizhiznennyy kontrol' regeneratsii slizistoy obolochki polosti rta posle fraktsionnogo lazernogo fototermoliza metodom krosspolarizatsionnoy opticheskoy kogerentnoy tomografii [Life-time control of oral mucosa regeneration after fractional laser photothermolysis using cross-polarization optic coherence tomography]. *Sovrem Tekhnol Med — Modern Technologies in Medicine* 2012; 2: 13–19.
22. Romanos G.E., Gladkova N.D., Feldchtein F.I., Karabut M.M., Kiseleva E.B., Snopova L.B., et al. Oral mucosa response to laser patterned microcoagulation (LPM) treatment. An animal study. *Lasers Med Sci* 2013 Jan; 28(1): 25–31.
23. Hantash B.M., Bedi V.P., Kapadia B., Rahman Z., Jiang K., Tanner H., et al. In vivo histological evaluation of a novel ablative fractional resurfacing device. *Lasers Surg Med* 2007 Feb; 39(2): 96–107.
24. Korzh N.A., Dedukh N.V. Reparativnaya regeneratsiya kosti: sovremennyy vzglyad na problemu. Stadii regeneratsii [Reparative bone regeneration: current view of the problem. Regeneration stages]. *Ortopediya, travmatologiya i protezirovaniye — Orthopedics, traumatology and prosthetic repair* 2006; 1: 77–84.
25. Mayborodin I.V., Drovosekov M.N., Toder M.S., Matveeva V.A., Kolesnikov I.S., Shevela A.I. Regeneratsiya povrezhdennoy kosti nizhney chelyusti krysa na fone vvedeniya autologichnykh mezenkhimal'nykh stvolovykh kletok kostnomozgovogo proiskhozhdeniya [Regeneration of rat damaged mandibular bone against the background of introduction of autologous mesenchymal stem marrow cells]. *Fundamental'nye issledovaniya — Fundamental Researches* 2011; 9: 264–269.
26. McDavid V.G., Cobb C.M., Rapley J.W., Glaros A.G., Spencer P. Laser irradiation of bone: III. Long-term healing following treatment by CO₂ and Nd:YAG lasers. *J Periodontol* 2001 Feb; 72(2): 174–82.
27. Friesen L.R., Cobb C.M., Rapley J.W., Forgas-Brockman L., Spencer P. Laser irradiation of bone: II. Healing response following treatment by CO₂ and Nd:Yag lasers. *J Periodontol* 1999 Jan; 70(1): 75–83.
28. Wang X., Zhang C., Matsumoto K. In vivo study of the healing processes that occur in the jaws of rabbits following perforation by an Er,Cr:YSGG laser. *Lasers Med Sci* 2005; 20(1): 21–27.
29. Queiroga A., Sousa F., Araújo J., Santos S., Sousa C.F., Quintans T., et al. Evaluation of bone repair in the femur of rats submitted to laser therapy in different wavelengths: an image segmentation method of analysis. *Laser Physics* 2008; 18(9): 1087–1091.